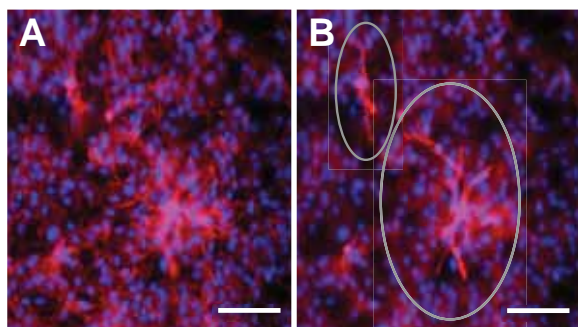
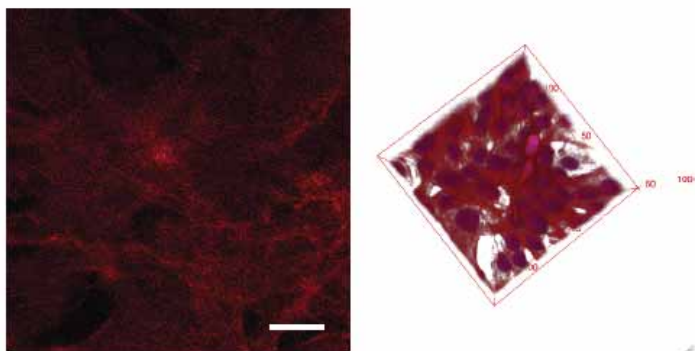


1  
2  
3  
4  
5  
6  
7  
8  
9  
10  
11  
12  
13  
14  
15  
16  
17  
18  
19  
20  
21  
22  
23  
24  
25  
26  
27  
28  
29  
30  
31  
32  
33  
34  
35  
36  
37  
38  
39  
40  
41  
42  
43  
44  
45  
46  
47  
48  
49  
50  
51  
52  
53  
54  
55  
56  
57  
58  
59  
60

## Supporting Information (Zeiger et al.)



**Supporting Figure S1 | Imaging of sprouting assays.** (A-B), Bovine retinal ECs, with fluorescent cell nuclei (blue, DAPI) and F-actin (red, Alexa-Fluor 594-labeled phalloidin). (A-B), Epifluorescence imaging was used to quantify number of sprouts, defined by (B), out of plane cellular sprouts (outlines in grey circles) extending from and contiguous with the (A), underlying cell monolayer (scale bar = 100  $\mu\text{m}$ ).



[3DSproutingMovieStack.avi](#) [3DSproutingMovieRotating.avi](#)

**Supporting movies 1-2 | Confocal videos of capillary endothelial sprouts** extending into overlaid gel. Animated z-stack (3DSproutingMovieStack.avi, Supp. Movie 1) and rendering of a sprout using 3D rotation (3DSproutingMovieRotating.avi, Supp. Movie 2) of a sprout shown in Supp. Figure 2. These movies are accessible by clicking on the movie snapshots above, which are hyperlinked to a dedicated Dropbox URL. Lateral scale bar shown = 20  $\mu\text{m}$ , and the vertical z-stack extends up to 52.6  $\mu\text{m}$ . These 3D renderings confirm the sprouted cells to be contiguous with the underlying monolayer. Sprout lengths included multiple cell lengths, e.g., 76.6  $\mu\text{m}$  for the sprout indicated in Fig. 3D of the main text.

Supporting movie files can be accessed for review via direct Dropbox links, due to file size:

**3DSproutingMovieStack** as .AVI (55MB) and .MP4 (1MB, lower resolution):

<https://www.dropbox.com/s/x3nv5mjwbvzb7e8/3DSproutingMovieStack.avi?dl=0>

<https://www.dropbox.com/s/bqk58ypvd2d3x6n/3DSproutingMovieStack.mp4?dl=0>

**3DSproutingMovieRotating** as .AVI (142MB) and .MP4 (4MB, lower resolution):

<https://www.dropbox.com/s/qrjctqfufzgo32j/3DSproutingMovieRotating.avi?dl=0>

<https://www.dropbox.com/s/ilpzahheeioyc0/3DSproutingMovieRotating%20copy.mp4?dl=0>

## Design and characterization of polydimethylsiloxane multiwell plates for application of tensile strain

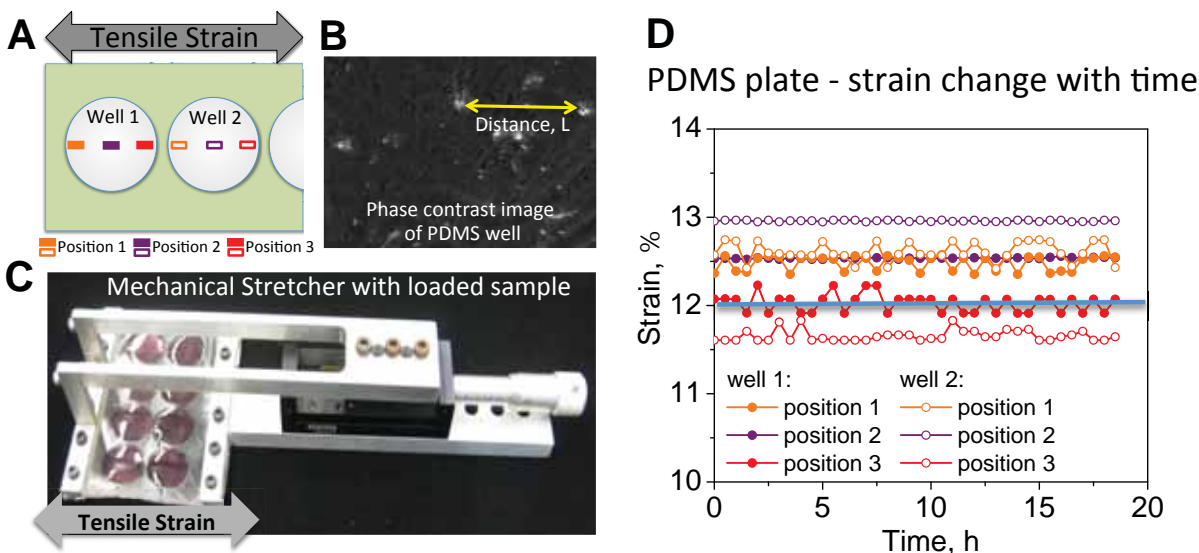
1  
2  
3  
4  
5  
6  
7  
8  
9  
10  
11  
12  
13  
14  
15  
16  
17  
18  
19  
20  
21  
22  
23  
24  
25  
26  
27  
28  
29  
30  
31  
32  
33  
34  
35  
36  
37  
38  
39  
40  
41  
42  
43  
44  
45  
46  
47  
48  
49  
50  
51  
52  
53  
54  
55  
56  
57  
58  
59  
60

Researchers have previously demonstrated that direct co-culture of mechanically coupled cell types, such as bovine adrenal cortex endothelial cells and bovine aortic smooth muscle cells, had a profound influence on endothelial cell proliferation and extracellular matrix production [1–3]. As has been observed for several adherent tissue cell types, vascular endothelial cell (VEC) adhesion efficiency is modulated by the stiffness of the substratum [4], and VEC proliferation and progression toward angiogenesis can be influenced by other mechanical stimuli such as fluid shear flow [5]. As outlined by Lee and Zeiger et al. [6], pericytes may alter the behavior of endothelial cells by modulating the mechanical properties of the basement membrane through contraction, or through direct strain effects on endothelial cells through cell-cell contacts, and thus alter neovascularization and angiogenesis. The approach outlined in our previous work, [6], allowed us to quantify the pericyte-generated contraction of a PDMS layer that was similar in thickness and stiffness to basement membrane, the substratum to which VECs adhere *in vivo* in blood vessels. We then endeavored to create a system in which we could apply that deformation directly to monolayers of VECs, in order to decouple this mechanical cue from other cues including biochemical concentrations. To do so, we required a multi-well format that could be mechanically strained to >10% static tensile strain for a range of replicated conditions, and ideally also be amenable to post-strain analysis such as immunocytochemical staining and optical microscopy.

For this multi-well strain format, PDMS was again chosen as the cell-culture substratum because the stiffness of this material can be tuned via the chemistry, and we reliably achieved static tensile strains of >25% without fracture of this elastomer. Only a few commercial “cell-stretchers,” such as STREX (B-Bridge International, Mountain View, CA) or FlexerCell (FlexCell International, Hillsborough, NC), are available. However, these devices are expensive and limited to proprietary components that can be difficult to incorporate into existing incubation microscopes for live cell imaging. Furthermore, devices such as FlexerCell do not allow for facile, direct optical imaging of cells during strain, and often create non-linearly elastic modes of deformation [7]. Thus, several researchers have developed and utilized customized cell stretching devices [8,9]. Based on these foundations, we developed an inexpensive, reproducible, *in vitro* uniaxial strain device (Fig. 1A in main text). All device parts were machined from aluminum with a fixed base attached to an extensible beam. We incorporated a commercial microstage with micrometer screws (and capability of motorization; Standa, LT) into the device base to accurately and precisely move the extensible beam to desired length increments away from the fixed base. This enabled manual extension to a prescribed engineering strain, calculated as  $\Delta L/L_0$  where  $\Delta L$  is the change in PDMS plate edge length between the two device arms and  $L_0$  is the original plate edge length. We end-clamped one end of the PDMS well plate to the fixed base and the opposite side to the extensible beam, via through-screws between the aluminum device arms. This device included a multi-well substrate format as to allow for multiple media and environmental conditions to be investigated under equivalent strain conditions. We designed an optically transparent mold that contained 16 wells of 1.25 cm diameter with a depth of 1.59 mm. We also tested other designs, such as 6-8 wells of 2.5 cm diameters, with similar success (data not shown).

We also experimentally confirmed uniformity of strain within a given well, and less than 3% variation about the mean magnitude of static engineering strain over durations up to 18 h, via timelapsd imaging of fiduciary markers in multiple wells. Figure S2B shows phase contrast

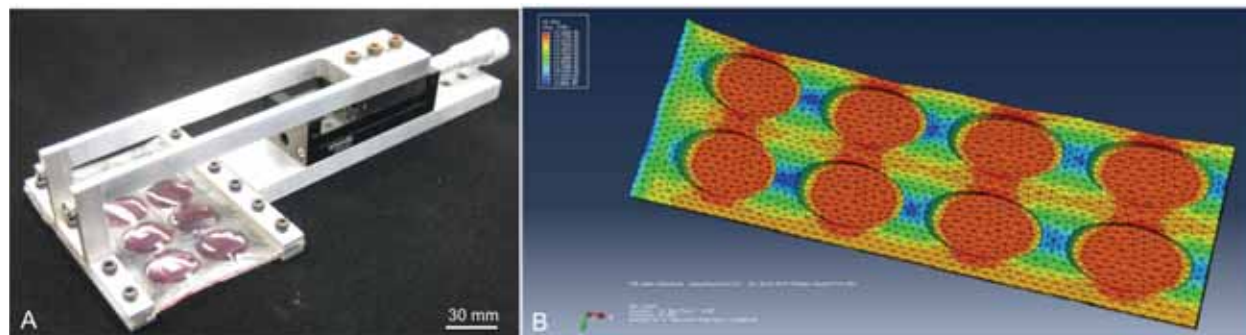
imaging of distinct points within a well to track changes in distance,  $L$ . These distances were tracked to determine strain at three distinct positions within two wells as schematically illustrated in Figure S2A. Figure S2C demonstrates the direction where 12% strain was applied to the elastomeric substrates. Data from these six positions were collected over the course 18 hours (Figure S2D). Strain across all positions did not deviate more than 1% from the applied engineering strain of 12%. At a given position, strain did not deviate more than 0.3%, which is less than 3% of variation from the applied strain of 12%. Together these data suggest that the applied engineering strain was transferred completely to the elastomeric substrate. Moreover, this tensile strain did not relax with time.



**Supporting Figure S2 | Stability and uniformity of tensile strain in the PDMS substrate applied with uniaxial stretching device.** (A) Schematic of three positions in the wells of the PDMS plate, where strain was measured; (B) Phase contrast image showing example of fiducial markers used to measure distance before,  $L_0$ , and after strain application,  $L$ , to determine strain in PDMS plate, calculated as  $\frac{L-L_0}{L_0} \cdot 100\%$ ; (C) Uniaxial stretching device with mounted plate; tensile strain is applied by increasing the distance between the arms holding the elastomeric plate; (D) Strain in PDMS plate and its changes over 18 h observation on microscope, at the positions shown in (A), in two different wells; blue line corresponds to 12% strain applied with device.

Design considerations based on analytical estimates and refined by finite element modeling of a hyperelastic multiwell plate demonstrated that true strain is uniform throughout the wells across the device. Figure S3 illustrates finite element modeling of polydimethylsiloxane (PDMS) molds under uniaxial strain, which indicated a uniform strain distribution across all wells. Device is typically 23.5 cm long and 12.7 cm wide, before the application of strain, and fits well within most common cell incubators (Fig. S3A). This simulation adopted an 8-well design of 1.9 cm diameter (Fig. S3B) because this design is anticipated to exaggerate any strain non-uniformities in larger well surface areas as compared with the smaller wells used in experiments within the manuscript. To identify any locations of non-uniform strain or interaction among wells upon application of uniaxial displacement, the multi-well PDMS strain device was modeled with finite element analysis (ABAQUS/Standard 6.10). PDMS was represented as an incompressible first-order Ogden hyperplastic material [13]. Displacement was applied along the x direction to achieve 25% engineering strain and

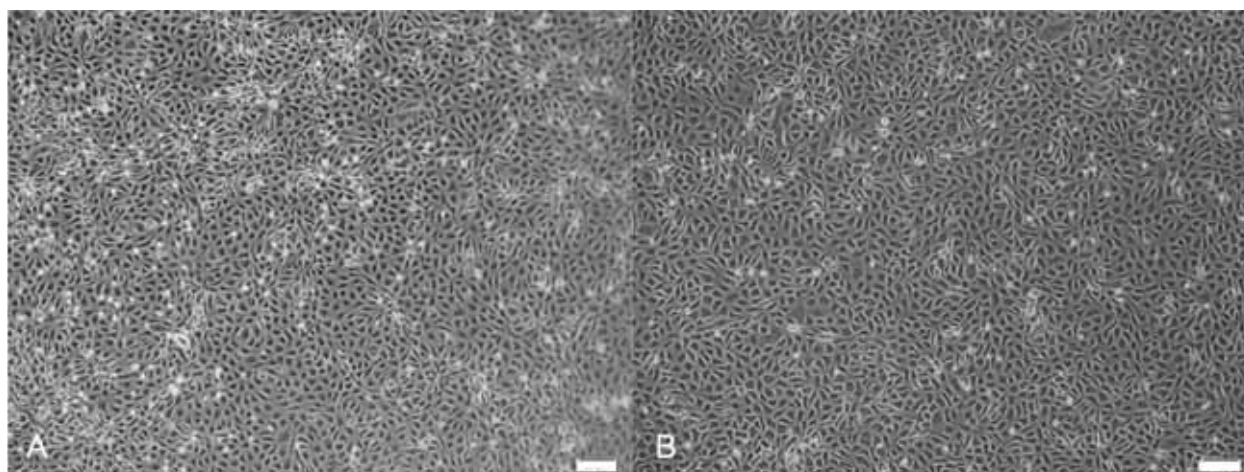
1  
2 symmetric boundary conditions along the x and y edges. We thus confirmed strains within wells  
3 ranging only 10% (of 25% strain) higher or lower than mean targeted strain (color variations  
4 within wells). This is in contrast with the non-uniform strain fields generated by devices such as  
5 FlexerCell [7].  
6



19 **Supporting Figure S3 | Finite element modeling of polydimethylsiloxane (PDMS) molds**  
20 **under uniaxial strain demonstrates a uniform strain distribution across all wells.** (A)  
21 Photograph of uniaxial strain device loaded with 8-well PDMS mold filled with Dulbecco's  
22 modified Eagle's growth medium. (B) Colored FEM simulation to identify any locations of non-  
23 uniform strain or interaction among wells upon application of uniaxial displacement. Strain  
24 applied was ~25% strain and is schematically represented as the color orange. Red represents  
25 maximum (~30%) strain where blue represents minimum (~1%) strain.  
26  
27

28 Notably, we altered the processing of this PDMS cell culture substratum to alleviate the  
29 need for surface functionalization with specific chemicals or proteins prior to cell seeding and  
30 adhesion (e.g., the deposition of chemical functional groups such as  $\text{NH}_2$  or  $\text{COOH}$ , or ECM  
31 proteins such as collagen or fibronectin). This allows for direct seeding of cells such as VECs,  
32 which upon adherence will produce ECM proteins that can adhere to the PDMS surface. Surface  
33 functionalization with specific functional groups may result in undesired effects on endothelial  
34 cell monolayer formation, and can significantly alter cell adhesion and behavior [10,11]. The  
35 present processing method creates hydrophilic PDMS cell culture surfaces with long-term  
36 stability for cell adhesion and growth. Surfaces remained hydrophilic (contact angle  $<45^\circ$ ) for  
37 longer than 14 days' immersion in fluid, comparable to that observed by Vickers et al. using a  
38 similar protocol for high-performance PDMS-based microchip electrophoresis [12].  
39  
40  
41

42 Surface roughness of the templates used to mold the wells was determined by atomic  
43 force microscopy to be  $370 \pm 53$  pm. This subnanometer-scale roughness was critical as  
44 topographical cues are known to play a significant role in guiding cell behavior [14]. Moreover,  
45 the optical transparency of these smooth well bottoms enabled phase contrast and  
46 epifluorescence imaging. Morphologically, bovine retinal endothelial cell (BREC) monolayers  
47 grown on these custom PDMS substrata are qualitatively identical to BRECs seeded onto  
48 traditional tissue culture polystyrene, or TCPS (SI Fig. S4). Thus, these multi-well plates can be  
49 considered a deformable, compliant analogue to TCPS, in the form of a "tissue-culture-PDMS"  
50 to which tissue cells can adhere and proliferate readily.  
51  
52  
53  
54  
55  
56  
57  
58  
59  
60



**Supporting Figure S4 | Monolayer Morphology.** Bovine retinal endothelial cell monolayers seeded directly onto (A) polydimethylsiloxane molds, processed as described in the text; and (B) tissue culture polystyrene, both at a seeding density of 100,000 cells/cm<sup>2</sup> and exhibiting similar morphologies.

This approach that applies uniaxial strain, in conjunction with this processing of PDMS for direct cell seeding, is unique to our knowledge. Others have previously created multi-well formats to uniaxially strain cell culture substrata [9], but still required subsequent surface adsorption with relevant biomolecules such as ECM or functionalized amino groups. Such surface modifications can alter cell physiology, independent of applied mechanical strain. Furthermore, we were able to utilize strain magnitudes exerted by relevant contractile cells, e.g., pericytes, *in vivo*, using our novel AFM-based substrate wrinkle analysis. This platform can easily be extended to incorporate computer-controlled actuation (e.g., by Standa Ltd.), to allow for both digitally controlled static, dynamic, or cyclic strain application in a multi-well format.

### **SI References**

- [1] Orledge A and D'Amore P A 1987 Inhibition of capillary endothelial cell growth by pericytes and smooth muscle cells. *J. Cell Biol.* **105** 1455–62
- [2] Sato Y, Tsuboi R, Lyons R, Moses H and Rifkin D B 1990 Characterization of the activation of latent TGF-beta by co-cultures of endothelial cells and pericytes or smooth muscle cells: a self-regulating system. *J. Cell Biol.* **111** 757–63
- [3] Sato Y, Okada F, Abe M, Seguchi T, Kuwano M, Sato S, Furuya A, Hanai N and Tamaoki T 1993 The mechanism for the activation of latent TGF-beta during co-culture of endothelial cells and smooth muscle cells: cell-type specific targeting of latent TGF-beta to smooth muscle cells. *J. Cell Biol.* **123** 1249–54
- [4] Thompson M T, Berg M C, Tobias I S, Rubner M F and Van Vliet K J 2005 Tuning compliance of nanoscale polyelectrolyte multilayers to modulate cell adhesion. *Biomaterials* **26** 6836–45
- [5] Liu W F, Nelson C M, Tan J L and Chen C S 2007 Cadherins, RhoA, and Rac1 are differentially required for stretch-mediated proliferation in endothelial versus smooth muscle cells. *Circ. Res.* **101**
- [6] Lee S, Zeiger A, Maloney J M, Kotecki M, Van Vliet K J and Herman I M 2010 Pericyte actomyosin-mediated contraction at the cell-material interface can modulate the microvascular niche. *J. Phys. Condens. Matter* **22** 194115
- [7] Vande Geest J P, Di Martino E S and Vorp D A 2004 An analysis of the complete strain

- 1 field within Flexercell™ membranes *J. Biomech.* **37** 1923–8
- 2
- 3 [8] Ahmed W W, Kural M H and Saif T A 2010 A novel platform for in situ investigation
- 4 of cells and tissues under mechanical strain *Acta Biomater.* **6** 2979–90
- 5
- 6 [9] Waters C M, Glucksberg M R, Lautenschlager E P, Lee C W, Van Matre R M, Warp R J,
- 7 Savla U, Healy K E, Moran B, Castner D G and Bearinger J P 2001 A system to impose
- 8 prescribed homogenous strains on cultured cells. *J. Appl. Physiol.* **91** 1600–10
- 9
- 10 [10] Miron-Mendoza M, Seemann J and Grinnell F 2010 The differential regulation of cell
- 11 motile activity through matrix stiffness and porosity in three dimensional collagen
- 12 matrices *Biomaterials* **31** 6425–35
- 13
- 14 [11] Keselowsky B G, Collard D M and García A J 2003 Surface chemistry modulates
- 15 fibronectin conformation and directs integrin binding and specificity to control cell
- 16 adhesion. *J. Biomed. Mater. Res. A* **66** 247–59
- 17
- 18 [12] Vickers J A, Caulum M M and Henry C S 2006 Generation of hydrophilic
- 19 poly(dimethylsiloxane) for high-performance microchip electrophoresis *Anal. Chem.*
- 20 **78** 7446–52
- 21
- 22 [13] Ogden R 1984 Non-linear elastic deformations *Eng. Anal. Bound. Elem.* **1** 119
- 23
- 24 [14] Zeiger A S, Hinton B and Van Vliet K J 2013 Why the dish makes a difference:
- 25 Quantitative comparison of polystyrene culture surfaces *Acta Biomater.* **9** 7354–61
- 26
- 27
- 28
- 29
- 30
- 31
- 32
- 33
- 34
- 35
- 36
- 37
- 38
- 39
- 40
- 41
- 42
- 43
- 44
- 45
- 46
- 47
- 48
- 49
- 50
- 51
- 52
- 53
- 54
- 55
- 56
- 57
- 58
- 59
- 60